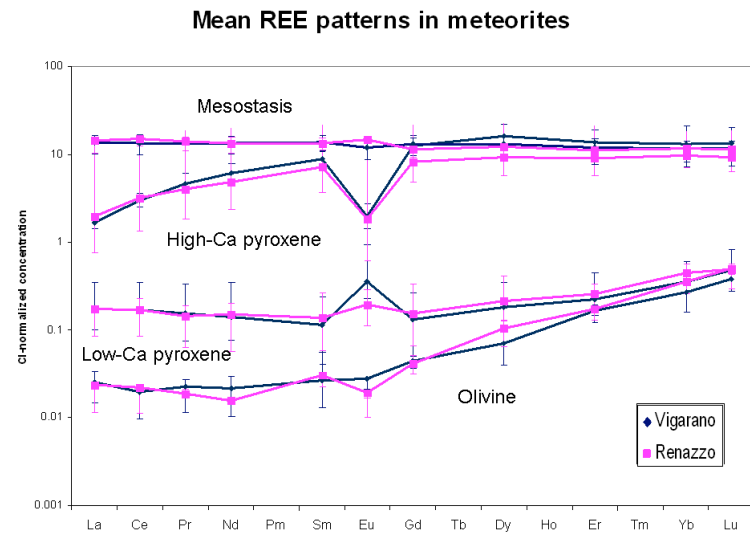


**TRACE ELEMENT MICRODISTRIBUTION IN CARBONACEOUS CHONDRITE CHONDRULES.** E. Jacquet<sup>1</sup>, M. Gounelle<sup>1</sup>, O. Alard<sup>2</sup>, <sup>1</sup>Laboratoire de Minéralogie et Cosmochimie du Muséum, Muséum National d'Histoire Naturelle, 57 rue Cuvier 75005 Paris, France (ejacquet@mnhn.fr). <sup>2</sup>Geosciences Montpellier, UMR5243, Université de Montpellier II, Montpellier, France.

**Introduction:** The nature of the chondrule-forming mechanism(s) is still controversial ([1]-[3]) and its elucidation requires clear cosmochemical constraints. Of particular importance are the nature of the precursors (dustballs, planetary debris [4] etc.), the thermal history [5], and whether chondrules formed as closed or open systems ([6]-[8]). Trace elements, with their diverse geochemical behaviors, offer unique insights on the conditions that governed their partitioning among the different phases. Former SIMS studies on ordinary chondrite chondrules ([9]-[11]) have concluded that olivine and pyroxene recorded rapid cooling rates of order 1000 K/h. Here, we present laser ablation inductively coupled plasma mass spectrometry (LA-ICP-MS) analyses of silicate phases in 36 carbonaceous chondrite chondrules and isolated olivine grains. Preliminary results from this study had been previously reported in [12] and [13].

**Methods:** Polished sections of Vigarano (CV3), Renazzo (CR2) and Acfer 187 (CR2) were examined using scanning electron microscopy and electron microprobe analyses. Chondrules representing a wide array of textures were selected for LA-ICP-MS analyses of olivine, low- and high-Ca pyroxene and mesostasis at University of Montpellier II. Spot size ranged from 25 to 100  $\mu\text{m}$ , with 50  $\mu\text{m}$  being a typical value. Signal was filtered using the GLITTER software, and, in combination with *a posteriori* SEM observations, allowed one to avoid compromising analyses with incompatible-element-rich inclusions. In order to further minimize the effects of possible contamination, a geometric averaging was used to produce means for each chondrule.

**Results:** Fig. 1 displays averaged Rare Earth Element (REE) concentrations for the different phases analyzed in Vigarano and Renazzo. Both meteorites exhibit essentially similar patterns. Mesostasis has a flat, if slightly increasing (with decreasing atomic number) REE pattern (with La spanning 6-22 x CI). Augites have a concave, negatively sloped pattern marked with negative Eu anomalies. Low-Ca pyroxene and olivine show depletion of light REE (LREE) relative to heavy REE (HREE), with HREE near chondritic values and La spanning 0.05-0.5 x CI for low-Ca pyroxene and 0.0008-0.15 x CI for olivine.



**Figure 1:** Average CI-normalized REE patterns for each phase in Vigarano and Renazzo. Error bars extend to the first and third quartiles.

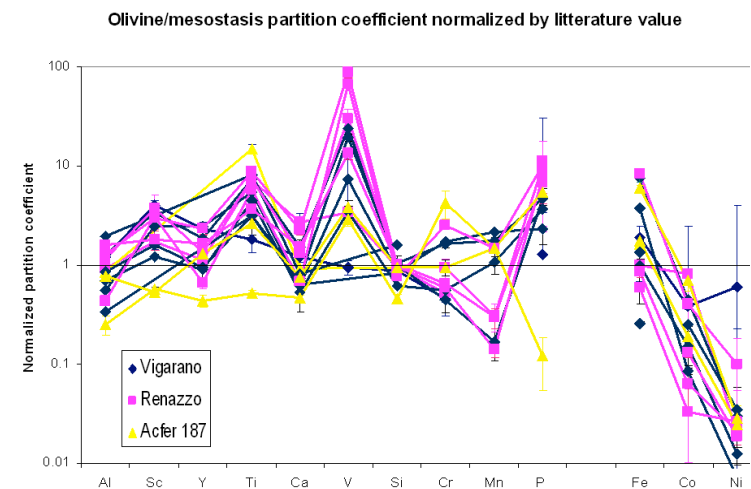


**Figure 2:** Olivine/mesostasis partition coefficients for a set of lithophile and siderophile elements, normalized by experimental values reported by [11]. A value of 1 thus corresponds to olivine/mesostasis equilibrium (under the conditions of the experiments). Each curve represents one chondrule, where the mean compositions for olivine and mesostasis have been used. Error bars are 1 standard deviation.

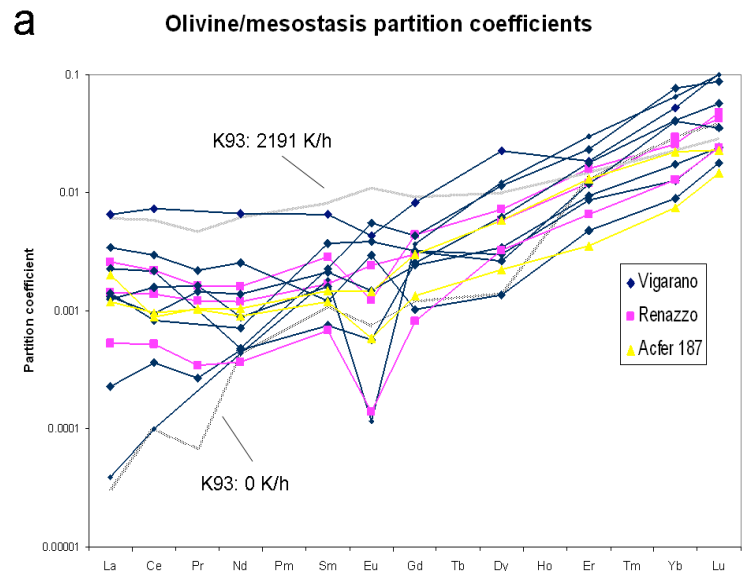
**Discussion:** If we use experimental partition coefficients compiled in [11], the hypothetical melt in equilibrium with olivine for our analyzed type I chondrules is too enriched in refractory, incompatible elements, by about one order of magnitude, to match bulk chondrule compositions [14], as was noted by [11] for ordinary chondrite chondrules. The mesostasis provides a better match for this melt, as checked in Fig. 2, save for probable redox effects (e.g. for V [11]). This suggests that most trace elements diffused efficiently throughout olivine crystals, as opposed to a fractional crystallization scenario (e.g. [11]). Using diffusion data of [15], this could indicate cooling rates slower than 1-100 K/h which may bridge the gap with those (0.5-50 K/h) estimated for igneous CAIs [16].

Fig. 3 shows olivine/mesostasis partition coefficients for REE. Similarly to [9]-[11], we note that olivine is generally more LREE-enriched than predicted by equilibrium partitioning and attribute this to kinetic effects [17]. This seems to be confirmed by the fact that the coarser the olivine crystals, the steeper the slope of their REE pattern, if coarse textures can be ascribed to protracted heating/cooling [18]. In particular, the two refractory forsterites analyzed obey equilibrium REE partitioning and are thus demonstrably igneous in nature [19].

Fig. 4 shows an anticorrelation between the concentration of Lu in low-Ca pyroxene and the mode of low-Ca pyroxene in the chondrule (which could account for the apparent discrepancy between [9] and [10]). This extends to other trace and minor elements (e.g. Al, Ca). We suggest that this could be understood in the framework of the model by [6] where pyroxene growth is a result of gas-melt interaction. Indeed, as mentioned by [6], this interaction adds silica to the melt, incurring a dilution of the other constituents, which dilution would also affect the resulting pyroxene. In this respect, it is interesting to note that the monoclinic structure of low-Ca pyroxene implies rapid cooling rates ( $> 100$  K/h; [20]), in contrast to the slow cooling rates inferred above to be recorded by olivine. This could corroborate the idea that the event that formed pyroxene was distinct from that which crystallized olivine.

**References:** [1] Ciesla (2005), *Chondrites & the protoplanetary Disk*, ASPC series, 341, 811. [2] Connolly & Desch (2004), *Chemie der Erde*, 64, 95-125. [3] Asphaug et al. (2011), *EPSL*, 308, 369-379. [4] Libourel & Krot (2007), *EPSL*, 254, 1-8. [5] Hewins et al. (2005), *Chondrites & the protoplanetary disk*, ASPC series, vol. 341, 286. [6] Libourel & Tissandier, (2006), *EPSL*, 251, 232-240. [7] Alexander et al. (2008), *Science*, 320, 1617-1619. [8] Hezel & Palme, (2007), *GCA*, 71, 4092-4107. [9] Alexander (1994), *GCA*, 58, 3451-3467. [10] Jones & Laynes (1997), *Am. mineralogist*, 82, 534-545. [11] Ruzicka et al. (2008), *GCA*, 72, 5530-5557. [12] Jacquet et al. (2009), *MAPS*, abstract #5354 (poster presentation). [13] Jacquet et al. (2010), *LPS XLI*, abstract #1533 (poster presentation). [14] Misawa & Nakamura (1988), *GCA*, 52, 1699-1710. [15] Chakraborty (2010), *Rev. in Mineralogy & Geochemistry*, 72, 603-609. [16] Apai et al. (2010), *Protoplanetary Dust*, 230-262. [17] Kennedy et al. (1993), *EPSL*, 115, 177-195. [18] Lofgren (1996), *Chondrules and the protoplanetary disk*, 187-196. [19] Pack et al. (2005), *GCA*, 69, 3159-3182. [20] Jones & Scott (1989), *LPSC proceedings.*, vol. 19, 523-536.

*gist*, 82, 534-545. [11] Ruzicka et al. (2008), *GCA*, 72, 5530-5557. [12] Jacquet et al. (2009), *MAPS*, abstract #5354 (poster presentation). [13] Jacquet et al. (2010), *LPS XLI*, abstract #1533 (poster presentation). [14] Misawa & Nakamura (1988), *GCA*, 52, 1699-1710. [15] Chakraborty (2010), *Rev. in Mineralogy & Geochemistry*, 72, 603-609. [16] Apai et al. (2010), *Protoplanetary Dust*, 230-262. [17] Kennedy et al. (1993), *EPSL*, 115, 177-195. [18] Lofgren (1996), *Chondrules and the protoplanetary disk*, 187-196. [19] Pack et al. (2005), *GCA*, 69, 3159-3182. [20] Jones & Scott (1989), *LPSC proceedings.*, vol. 19, 523-536.



**Figure 3:** Olivine/mesostasis partition coefficients for REE. Also plotted are experimental values by [17] (“K93”).

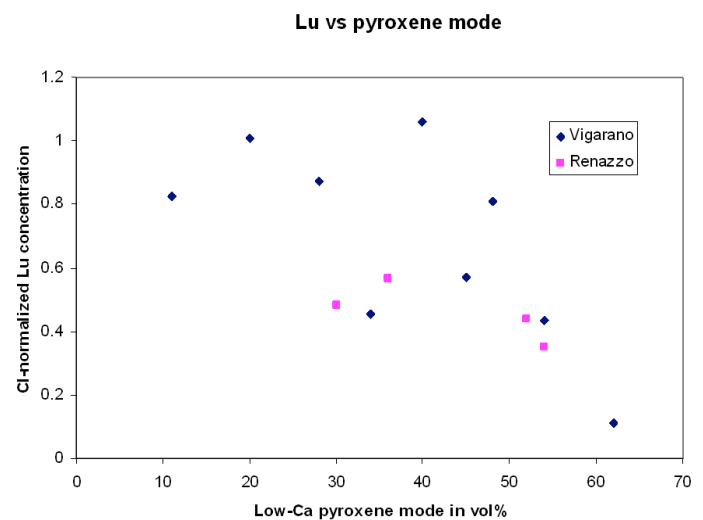


**Figure 4:** Plot of Lu concentration in low-Ca pyroxene vs low-Ca pyroxene mode in each chondrule.